

# Material instabilities in the $TaO_x$ -based resistive switching devices (Invited)

M. Skowronski

Dept. Materials Science and Engineering  
Carnegie Mellon University  
Pittsburgh, PA 15213, USA

Phone: (1)-(412)-268-2710, email: mareks@cmu.edu

**Abstract**— Oxide-based resistive switching devices offer an attractive set of characteristics for embedded memories and neuromorphic computing. However, their endurance is limited with the origin of failure mechanisms not firmly established. Transmission electron microscopy results on TiN/TaO<sub>x</sub>/TiN structures suggest that the primary reason is the intrinsic instability of TaO<sub>x</sub> in the middle of the composition range. This material separates into Ta- and O-rich phases that affect the filament morphology and can result in either stuck-in-high or stuck-in-low resistance state failure. An additional factor affecting endurance of switching devices is the interdiffusion at the electrode-functional oxide interfaces.

**Index Terms**—non-volatile memory devices, reliability, interdiffusion, transmission electron microscopy.

## I. INTRODUCTION

The highest value of endurance reported for transition metal oxide-based resistive switching devices reported so far was in the  $10^{10}$ - $10^{12}$  range [1][2]. The endurance of ReRAM in production offered by TSMC is only  $10^4$  [3]. While this number is comparable with endurance of FLASH, it severely limits the possible ReRAM applications. This warrants a detailed study of the failure mechanisms.

A standard model for the functioning of ReRAM device is that the initially uniform device undergoes a one-time electroforming procedure during which the oxygen ions in the oxide are forced by the applied electric field to cross the boundary between the functional layer and the anode [4]. This creates oxygen vacancies in the oxide which act as shallow donors and make the oxide n-type. For unspecified reason, this process is thought to be localized creating a small conducting filament connecting the electrodes. Application of bias with opposite polarity creates the gap in the filament and increases the resistance.

Some authors suggest that the switching process relies on the repeated transfer of oxygen ions from the functional layer to the electrode creating low resistance state (LRS) and back

creating the high resistance state (HRS) [5]. Modifications of this model suggest that the filament can be formed only at elevated temperatures induced by threshold switching [6], by motion of both metal and oxygen ions [7][8], by the lateral motion of both due to temperature gradient [9], and different combinations of the above.

ReRAM devices fail by two distinct failure modes. One is the failure by stuck-in-LRS interpreted as due to formation of a “strong”, highly conducting filament with high Ta/O ratio and/or large diameter [10][10]. This is a natural interpretation if switching events repeatedly induce transfer of oxygen to electrodes and accumulation of oxygen vacancies. However, almost as likely is the failure by stuck-in-HRS mode in which the gap cannot be bridged by mobile ions [11].

This work addressed the failure modes by transmission electron microscopy of functioning and failed TiN/TaO<sub>x</sub>/TiN devices. Of particular importance is the morphology of the conducting filament and intermixing at the functional oxide / electrode interfaces.

## II. EXPERIMENTAL

Devices used in this work were consisted of sputtered 40 nm TiN / 50 nm TaO<sub>x</sub> / 30 nm TiN sandwich structures with the lateral size of the active area of 150 nm (schematic diagram shown in Figure 1(a)). The devices were specifically designed to allow for elemental mapping of the filament. The particular difficulty is locating the filament which can form at small nonuniformities of as-fabricated structures such as density changes due to deposition on patterned substrates. These were eliminated by deposition of a planar structure with only the patterned top electrode. As the consequence, the filament always formed in the middle of the device with the microscopy sample yield over 80%. Also, the best contrast of the [Ta]/[O] ratio can be achieved using High Angle Annular Dark Filed modality of the transmission electron microscopy (TEM). In order to enhance this contrast, the only heavy element in the structure was Ta in TaO<sub>x</sub> functional layer. All local changes in the Ta content are then due to redistribution of Ta within the oxide. Figure 1(b) shows the TEM bright field image of as-fabricated device.

Sponsored by NSF grant DMR 2208488

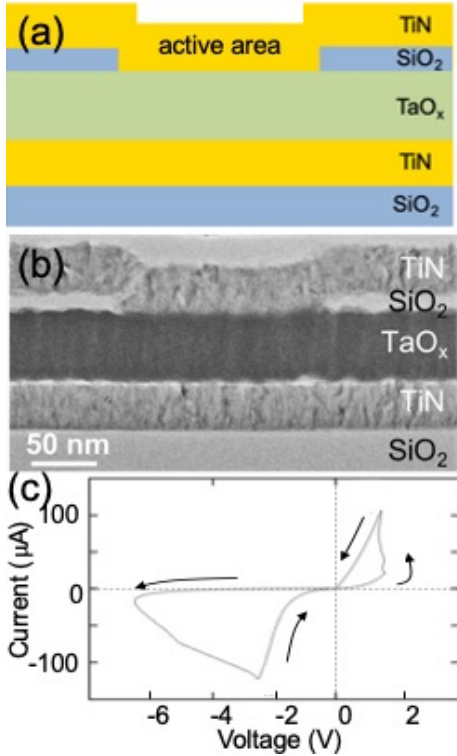


Figure 1 (a) Schematic diagram of the device structure. (b) cross-section TEM bright field image of as-fabricated device. (c) Switching I-V characteristics.

Devices at about 5V during the quasi-static voltage sweep and current of 0.2 mA. All devices were protected against capacitive discharge during formation and switching by an integrated on-chip 50 kOhm load resistor. Switching voltages and currents were 2V and 100  $\mu$ A, respectively.

### III. RESULTS AND DISCUSSION

Figure 1 shows two cross-sectional transmission electron microscopy images of the same TiN/TaO<sub>x</sub>/TiN device that was just electroformed with positive bias applied to the top electrode and left in the HRS. Panel (a) shows the High Angle Annular Dark Field image. The dark areas on top and bottom correspond to TiN electrodes with the grey area in the middle representing the functional oxide. HAADF images were formed by the electrons transmitting through the sample and scattering at angle exceeding 50 mrad from the optical axis of the microscope. The scattering is caused by the interaction with atomic nuclei with the probability proportional to the square of the atomic number. Since the structure was intentionally designed with the only heavy element being Ta (Z=73), contributions from the remaining atoms (N (Z=7), O (Z=8), and Ti (Z=22) are an order of magnitude or more, lower. In essence, the image intensity could be interpreted as in its entirety due to the number of Ta atoms in a given thickness of the sample. The bright contrast in the middle of the image represents the local accumulation of Ta [12]. This interpretation is supported by the image in Figure 1(b) which

shows the intensity distribution of the X-ray M-line of Ta (X-ray Energy Dispersive Spectroscopy (XEDS)). The two images are identical in all essential details. Since the signal to noise ratio in HAADF is much better than that in Ta-XEDS maps, I will focus on HAADF images to discuss distribution of tantalum in the remainder of this report.

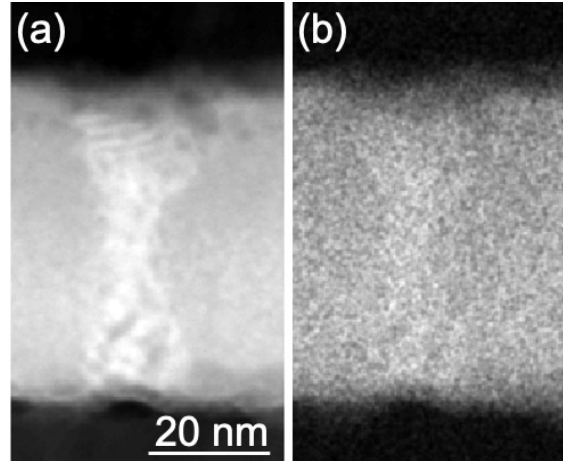


Figure 1 (a) HAADF cross-sectional image of the device electroformed in positive polarity. (b) The same sample imaged by XEDS using the M-line of Ta.

This and other filaments in as-formed devices share number of characteristic features. All exhibit Ta-enriched core with roughly cylindrical shape and 10-20 nm diameter. The increased Ta content of the core is due to the motion of Ta ions laterally toward the center of the filament and is caused by the radial temperature gradient in the device. Both HAADF and XEDS images show a Ta-depleted gap region close to the anode in the electroformation process. Since the as-deposited TaO<sub>x</sub> film had approximately TaO<sub>2</sub> composition and the gap had the darker contrast, this indicated composition approaching TaO<sub>2.5</sub>. One should note that the contrast within the filament varies in brightness pointing to varying local compositions.

Figure 2 shows three more HAADF images of as-electroformed devices. Structure in panel (a) was formed in positive polarity while that in panels (b) and (c) in negative one. Accordingly, the filament in (b) and (c) exhibits a gap located at the interface with the bottom electrode. All four HAADF images above show the intensity variation in the filament core consisting of darker, typically elongated spots on the bright background. In some of the dark spots, the signal intensity is lower than that of the surrounding oxide indicating lower Ta content than in the initially deposited film. This observation is apparently in opposition to the net accumulation of Ta in the core of the filament. The reason for inhomogeneous TaO<sub>x</sub> composition is the intrinsic instability of TaO<sub>x</sub> in the middle of the composition range. The only two stable solids in the Ta-O system below 1300 °C are TaO<sub>2.5</sub> and Ta with very narrow existence range of TaO<sub>2.5</sub> and about 5% solubility of oxygen in Ta [13]. For the compositions in

between, the oxide should decompose into Ta- and O-rich phases. This can occur through the nucleation or through the spinodal decomposition. In the first case the resulting phases would essentially be metallic Ta and  $TaO_{2.5}$ . In the second, the resulting compositions can be different. It is difficult to ascertain the composition variation shown in the HAADF micrographs due to the size of segregated regions ( $<5$  nm) which is much smaller than the thickness of the TEM sample. Some insights can be gained from the plan view images.

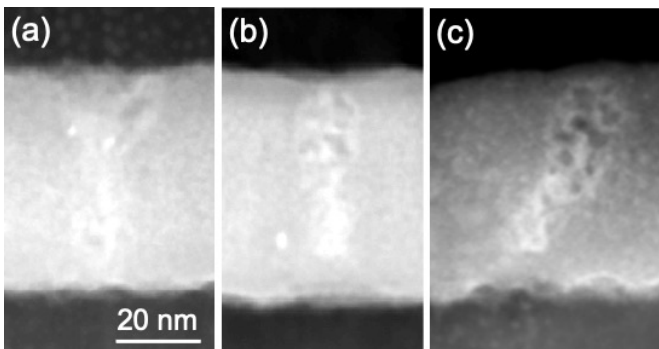


Figure 2. HAADF images of the filament in device formed in positive polarity (a) and negative polarity (b) and (c).

HAADF image of the filament in Figure 3 shows a bright contrast circle with the diameter of about 35 nm. The bright core is surrounded by the dark ring with diameter of about 80 nm. The bright and dark areas in the core have size of about 4 nm with bright areas much brighter and Ta depleted areas being darker than the surrounding oxide. The size of the segregated areas decreases rapidly with distance from the center. As the current primarily flows thought the Ta-rich core, the temperature drops rapidly with distance from the center. Accordingly, the ability of ions to diffuse and segregate decreases as well resulting in decrease of the feature size. Nucleation is a relatively rare event requiring large deviation from the average composition over a small volume. On the other hand, the spinodal decomposition occurs uniformly throughout the entire material with both the amplitude of the composition change and its wavelength increasing with time at temperature. The image in Figure 3 is therefore consistent with spinodal decomposition.

It is worth considering the consequences of this  $TaO_x$  instability. In either case of nucleation and growth and spinodal decomposition, the initially small deviations from the average composition grow. The segregation induced by the gradient of chemical potential is in addition to other forces acting on ions such as that of electric field, temperature gradient, and stress. If, for example temperature gradient locally causes increase of Ta content, the phase separation will enhance this effect. Similarly, the depletion of Ta will be heightened. In other words, the tendency to form the filament will be spontaneously accelerated. The effect on stability is more complex.

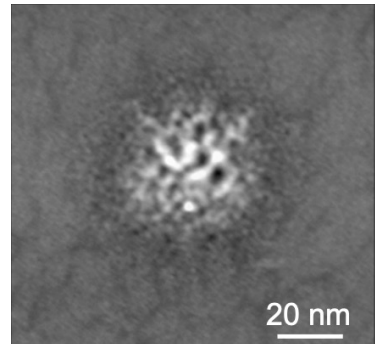


Figure 3. HAADF plan view image of the lower part of the filament formed in positive polarity.

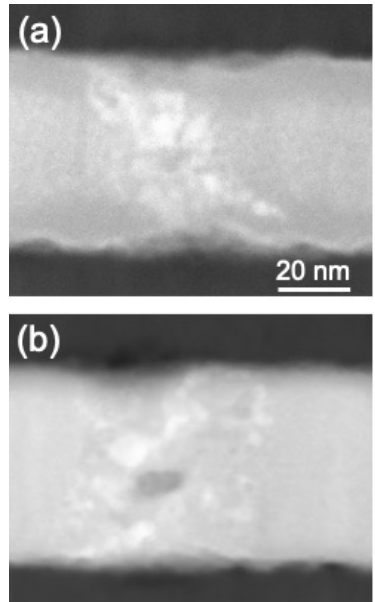


Figure 4. HAADF images of two devices at the end of endurance test after  $10^5$  switching cycles.

The changes in the filament with repeated switching and its structure at the end of endurance ( $\sim 10^5$  cycles) are shown in Figure 5. The devices in both panels have been formed in positive polarity with the gap located at the top electrode. Similarly as in just electroformed devices, there was only one filament in each device. Its diameter, however, was greatly increased to 40-60 nm. Most of the filament had enhanced Ta content with the grainy contrast seen in Figures 1 through 4. It is apparent that the phase separation continued with repeated switching [14]. There was no obvious gap Ta-depleted gap or a continuous bright path connecting the electrodes. For the sake of the discussion, let us assume that the electroformation produced a Ta-rich uniform cylinder connecting the electrodes. If there are two small statistically appearing maxima along the length, the phase separation would tend to produce the Ta ion flux toward the maxima and could break the filament. It appears that this phenomenon makes the filament intrinsically unstable.

An additional instability of ReRAM structures is common to all electronic devices: all such structures are far from equilibrium containing materials with different compositions in close proximity. In ReRAM this instability is enhanced by high temperatures in the filament and amorphous structure of the functional oxide leading to high diffusivities. The elemental map of oxygen distribution by XEDS in device shown in Figure 1 is displayed in Figure 5 with the HAADF image in panel (b) for comparison. One can see a slight decrease of the oxygen signal at the location of the filament. More importantly, there is a lighter grey area across the interface with TiN marked by an arrow indicating in-diffusion of oxygen. The area has the shape of the disc segment with height of  $\sim 8\text{nm}$ , cord length of  $\sim 30\text{ nm}$ , and oxygen concentration up to 50%. There is no sign of interdiffusion at the interface with the bottom electrode for oxygen or any other element.

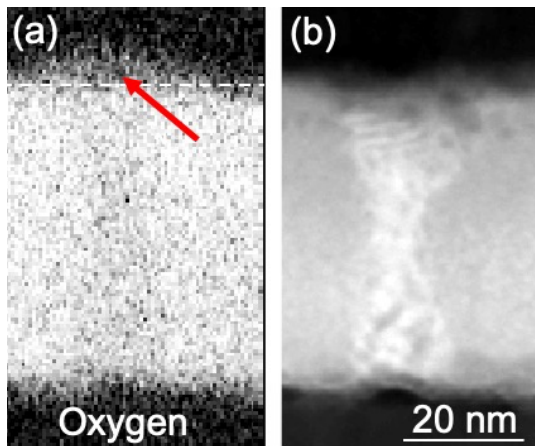


Figure 5 (a) XEDS oxygen map of device shown in Figure 1. Arrow points the oxygen diffusion in TiN. (b) HAADF image of the same device to serve as a reference.

Figure 6 shows the line profiles of elemental content along the centerline of the filament (blue line) starting at the middle of the oxide layer. The profile marked in red was collected away from the filament and serves as the reference for as-fabricated distribution. The first panel shows the Ta profile with the distinct dip of the Ta constant at the interface with the anode and no sign of Ta interdiffusion into TiN. Oxygen profile in the filament is significantly above that of the reference and extends about 50 nm into the TiN. Nitrogen appears to be depleted in TiN close to the interface (being replaced by oxygen) and ti diffused out of TiN and into  $\text{TaO}_x$ . The likely reason for the asymmetry of the two interfaces is the location of the gap. In this device the gap was located next to the top electrode resulting in the highest temperatures along the filament. The estimates of the temperatures within the gap for the dissipated power level used in switching are in the 1000  $^{\circ}\text{C}$  range. They are about 300  $^{\circ}\text{C}$  higher than the temperatures at the interface with bottom electrode.

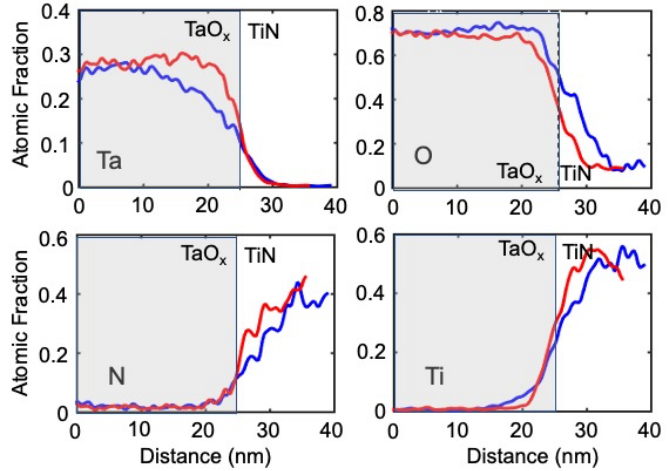


Figure 6. Line profiles of Ta, O, N, and Ti concentrations across the interface with the top electrode in device shown in Fig. 1.

There are two driving forces behind the exchange of ions: electric field and chemical potential gradient. Many authors suggested that it is the electric field that is dominant and can work even without much temperature increase. Such mechanism of intermixing would be consistent with oxygen and Ti crossing the interface. However, as the field does not extend into the electrode, the oxygen motion up to 5 nm into TiN has to be explained as driven by concentration gradient. Also, nitrogen moving from TiN and into  $\text{TaO}_x$  is moving against the field. One can conclude then, that the intermixing at the ReRAM interfaces is primarily caused by the Fick's diffusion process allowed by the high temperatures within the filament. The intermixing in devices at the end of endurance is comparable to interdiffusion after formation with the exception of interdiffusion occurring at both interfaces.

In summary, the TEM analysis of just formed and failed devices shows fine structure of the filament composed of Ta- and O-rich areas with size between 2-5 nm. The effect appears to be due to phase separation and can lead to accelerated formation of the conductive filament as well as its dissociation into disconnected Ta-rich inclusions. The phase separation continues with repeated switching leading to increased diameter of the filament. High temperatures with the filament result in interdiffusion between functional oxide and the electrodes. It will be critical to limit the dissipated power and temperature excursions to achieve improved endurance.

#### IV. ACKNOWLEDGMENTS

I would like to acknowledge my Ph. D. student contributions: Yuanzhi Ma, Jonathan M. Goodwill, and Jingjia Meng.

#### V. REFERENCES

- [1] M. J. Lee *et al.*, “A fast, high-endurance and scalable non-volatile memory device made from asymmetric  $\text{Ta}_2\text{O}_{5-x}/\text{TaO}_{2-x}$  bilayer structures,” *Nat. Mater.*, vol. 10, no. 8, pp. 625–630, Jul. 2011.
- [2] Y. Y. Chen *et al.*, “Endurance/Retention Trade-off on  $\text{HfO}_2$

Cap 1T1R Bipolar RRAM,” *IEEE Trans. Electron Dev.*, vol. 60, no. 3, pp. 1114–1121, Feb. 2013.

[3] P. Clarke, “TSMC offers 22 nm RRAM, taking MRAM on to 16 nm,” *ee news*, p. August 25, 2020.

[4] R. Waser, R. Dittmann, G. Staikov, and K. Szot, “Redox-Based Resistive Switching Memories - Nanoionic Mechanisms, Prospects, and Challenges,” *Adv. Mater.*, vol. 21, no. 25–26, pp. 2632–2663, Jan. 2009.

[5] D. Cooper *et al.*, “Anomalous Resistance Hysteresis in Oxide ReRAM: Oxygen Evolution and Reincorporation Revealed by In Situ TEM,” *Adv. Mater.*, vol. 29, no. 23, pp. 1700212–1700218, Apr. 2017.

[6] A. A. Sharma, M. Noman, M. Abdelmoula, M. Skowronski, and J. A. Bain, “Electronic Instabilities Leading to Electroformation of Binary Metal Oxide-based Resistive Switches,” *Adv. Funct. Mater.*, vol. 24, no. 35, pp. 5522–5529, Jul. 2014.

[7] A. Wedig *et al.*, “Nanoscale cation motion in  $TaO_x$ ,  $HfO_x$  and  $TiO_x$  memristive systems,” *Nat. Nanotechnol.*, vol. 11, no. 1, pp. 67–74, Jan. 2016.

[8] Y. Ma *et al.*, “Formation of the Conducting Filament in  $TaO_x$ -Resistive Switching Devices by Thermal-Gradient-Induced Cation Accumulation,” *ACS Appl. Mater. Interfaces*, vol. 10, no. 27, pp. 23187–23197, Jun. 2018.

[9] J. Meng, E. Lian, J. D. Poplawsky, and M. Skowronski, “Modeling of the Thermodiffusion-Induced Filament Formation in  $TiN/Ta_xO_{1-x}/TiN$  Resistive-Switching Devices,” *Phys. Rev. Appl.*, vol. 17, p. 054040, 2022.

[10] P. Huang *et al.*, “Analytic model of endurance degradation and its practical applications for operation scheme optimization in metal oxide based RRAM,” *2013 IEEE Int. Electron Devices Meet.*, pp. 597–600, 2013.

[11] C. Y. Chen *et al.*, “Endurance degradation mechanisms in  $TiN/Ta_2O_5/Ta$  resistive random-access memory cells,” *Appl. Phys. Lett.*, vol. 106, no. 5, pp. 2–4, 2015.

[12] Y. Ma *et al.*, “Stable Metallic Enrichment in Conductive Filaments in  $TaO_x$ -Based Resistive Switches Arising from Competing Diffusive Fluxes,” *Adv. Electron. Mater.*, vol. 1800954, pp. 1–8, 2019.

[13] S. P. Garg, N. Krishnamurthy, A. Awasthi, and M. Venkatraman, “The O-Ta (Oxygen-Tantalum) system,” *J. Phase Equilibria*, vol. 17, no. 1, pp. 63–77, Jan. 1996.

[14] Y. Ma, P. P. Yeoh, L. Shen, J. M. Goodwill, J. A. Bain, and M. Skowronski, “Evolution of the conductive filament with cycling in  $TaO_x$ -based resistive switching devices,” *J. Appl. Phys.*, vol. 128, no. 19, 2020.